coatings

MDPI

Article

Active Biodegradable Polyvinyl Alcohol–Hemicellulose/Tea Polyphenol Films with Excellent Moisture Resistance Prepared via Ultrasound Assistance for Food Packaging

Yining Wang [1], Jinhui Li [1], Xin Guo [1], Haisong Wang [1], Fang Qian [2,*] and Yanna Lv [1,3,*]

[1] School of Light Industry and Chemical Engineering, Dalian Polytechnic University, Dalian 116034, China; yiningwangdlpu@163.com (Y.W.); lijinhui0467@163.com (J.L.); gx9255@163.com (X.G.); wanghs@dlpu.edu.cn (H.W.)
[2] School of Food Science and Technology, Dalian Polytechnic University, Dalian 116034, China
[3] State Key Laboratory of Pulp and Paper Engineering, South China University of Technology, Guangzhou 510640, China
* Correspondence: qf09@163.com (F.Q.); lvyn@dlpu.edu.cn (Y.L.); Tel.: +86-0411-8632-3509 (Y.L.)

Abstract: Poor water-vapor barriers and mechanical properties are common problems of biobased films. To maintain food quality, the barrier and its strength performance need to be improved. Tea polyphenols (TP) are a natural active substance, and their benzene ring structure provides a barrier for them as a film material. Films that incorporate TP also have enriched functionalities, e.g., as antioxidants. Here, active poly (vinyl alcohol) (PVA)-hemicellulose (HC)/TP films with good moisture resistance and antioxidant capacity were prepared via ultrasound assistance. The effects of TP incorporation and ultrasonication on the physical, antioxidant, and micromorphological properties of the films were investigated. Results showed that the addition of TP improved the thermal stability and water-vapor permeability (WVP) of the composite films. When a PVA-HC/TP composite film with a PVA-HC to TP mass ratio of 100:10 was treated with ultrasonication for 45 min, tensile strength was 25.61 Mpa, which was increased by 54% from the film without any treatment, and water-vapor permeability (WVP) value declined from 49% to 4.29×10^{-12} g·cm/cm^2·s·Pa. More importantly, the films' DPPH scavenging activity increased to the maximal levels of 85.45%. In short, these observations create a feasible strategy for preparing high-performance biodegradable active-packaging films.

Keywords: ultrasonication; hemicellulose; tea polyphenol; polyvinyl alcohol; active film

check for updates

Citation: Wang, Y.; Li, J.; Guo, X.; Wang, H.; Qian, F.; Lv, Y. Active Biodegradable Polyvinyl Alcohol–Hemicellulose/Tea Polyphenol Films with Excellent Moisture Resistance Prepared via Ultrasound Assistance for Food Packaging. *Coatings* **2021**, *11*, 219. https://doi.org/10.3390/coatings11020219

Academic Editor: Gianni Zoccatelli

Received: 14 December 2020
Accepted: 5 February 2021
Published: 12 February 2021

1. Introduction

Because of the significant environmental concerns and consumer health, novel biomass-based packaging materials are attracting much research attention. Film products from natural sources such as polysaccharides, proteins, and lipids were investigated in several studies in recent years [1–6]. Hemicellulose (HC), as a promising renewable raw material source, is considered to be the second most abundant natural polysaccharide after cellulose, with excellent biocompatibility, biodegradability, and reproducibility, providing the possibility to develop packaging materials [7–9]. However, previous studies showed that films made by purified hemicellulose have weak film-forming properties and worse tensile strengths. One common method for improving functional properties of films is to mix other polymers with hemicellulose [10]. Poly(vinyl alcohol) (PVA) is a biocompatible synthetic polymer that is commonly used in drug synthesis, paper coating, and packaging materials because of its excellent film-forming, adhesive, and transparent properties [11–14]. Because PVA contains hydroxyl groups, it is most likely to react with hemicellulose owing to the formation of hydrogen bonds [15–17].

Recently, there has been increasing interest in using tea polyphenol (TP) as a natural antioxidant or antimicrobial component in the food industry due to its low cost, nontoxic

nature, abundance, and biocompatibility. TP is a mixture of catechins extracted from tea or agricultural waste [18,19]. The antioxidant mechanism is primarily due to the ability of polyphenols to trap reactive oxygen species and chelating metal ions [20–23]. Despite previous studies having reported antioxidant films containing TP [24–27], the incorporation of TP into composite films by physical blending could lead to the poor dispersion of TP in a film matrix [18,28,29]. Ultrasound is low-cost, effective, and nonpolluting. The physical effects of ultrasound are primarily due to cavitation, which is the breakdown of microbubbles that burst and disperse as a sound wave through the solution. Thus, ultrasound results in a uniform distribution of the particles in the solution on a macroscopic scale, whereas the cavitation effect further homogenizes the particles on a microscopic scale [30,31]. Several studies were performed on the film preparation with ultrasonic radiation. Wang et al. reported that ultrasound treatment reduced particle size and film-forming solution viscosity, and improved the compatibility of chitosan films with rice protein hydrolysates [32]. Liu and colleagues investigated the impact of ultrasonic treatment on the properties of films based on sweet-potato starch, indicating that, after ultrasonic treatment, film-forming components became more compatible [33].

The above show that tea polyphenols are an outstanding antioxidant used in active packaging, and ultrasound assistance is an effective method to achieve film-forming component compatibility compared with physical blending without any pretreatment. To the best of our knowledge, active films based on polysaccharide-based films carrying TP prepared via ultrasound assistance have not yet been reported. Our hypothesis is that there are synergistic effects between TP and ultrasonication for further improving film performance. Therefore, on the basis of our previous study that combined the advantages of polyvinyl alcohol and hemicellulose to develop poly (vinyl alcohol) (PVA)-hemicellulose (HC) films [34], we attempted to add tea polyphenols to a PVA–HC matrix with ultrasonic assistance. Impacts of TP content and ultrasound existence on film performance were investigated by Fourier transform infrared spectroscopy (FT-IR), atomic force microscopy (AFM), X-ray diffraction (XRD), thermal analysis, and DPPH free radical scavenging. Subsequently, the duration of the ultrasound on moisture resistance and mechanical properties was tested. Results are useful in understanding the role of ultrasonication in improving the performance of hemicellulose-based films.

2. Materials and Methods

2.1. Materials

Hemicellulose was extracted from sugarcane bagasse pith using an ultrasound-assisted alkaline method according to our previous report [35]. PVA-1799 (alcoholysis degree = 99%; Mw = 75,000 g/mol) was purchased from Sinopharm Chemical Reagent Co., Ltd. (Shanghai, China). TP, with polyphenol content >98% and catechin content >90%, was supplied by Darui Fine Chemicals co., Ltd. (Shanghai, China). Sorbitol was purchased from Komeio Chemical Reagent Co., Ltd. (Tianjin, China). 1,1-Diphenyl−2-picrylhydrazyl radical 2,2-diphenyl−1-(2,4,6-trinitrophenyl)hydrazyl (DPPH) (98% purity) was obtained from Yuanye Biological Technology Co., Ltd. (Shanghai, China).

2.2. Film Preparation

The film preparation process is simply illustrated in Scheme 1. All films were prepared by the solution-casting method; 1.6 g PVA was dissolved into 20 mL deionized water at 95 °C for 1 h to obtain the PVA solution. Subsequently, 0.4 g hemicellulose was added to the PVA solution at 75 °C for 1 h, and 0.4 g sorbitol was then added as the plasticizer and stirred for 30 min. TP (0%, 1%, 5%, 10% *w/w* based on PVA and HC total solids weight) was added to the PVA–HC solution and stirred for 30 min. The effect of the ultrasound on the film-forming properties was checked. To detect the effect of the ultrasound on TP dispersion, each solution was treated with ultrasound in an SK2510 HP ultrasonic bath (Kudos, China) at an ultrasonic frequency of 53 kHz for 0, 15, 30, and 45 min, respectively. After that, each solution was stirred again at 75 °C for 30 min. Lastly, the film solution

was poured onto a ZAA 2300 automatic coating machine (Zehntner, Switzerland) to scrape the film onto the acrylic sheet, and then placed in an oven at 30 °C for 12 h. The dried film samples were peeled off and stored at 25 °C and 50% RH for 48 h for further analysis. The obtained films were marked systematically, for example, TP10-45 (TP: PVA-HC = 10%, mass ratio, ultrasonic processing for 45 min). The formula of each film is shown in Table S1. All film samples were stored at 25 °C and 50% RH for 48 h for further analysis.

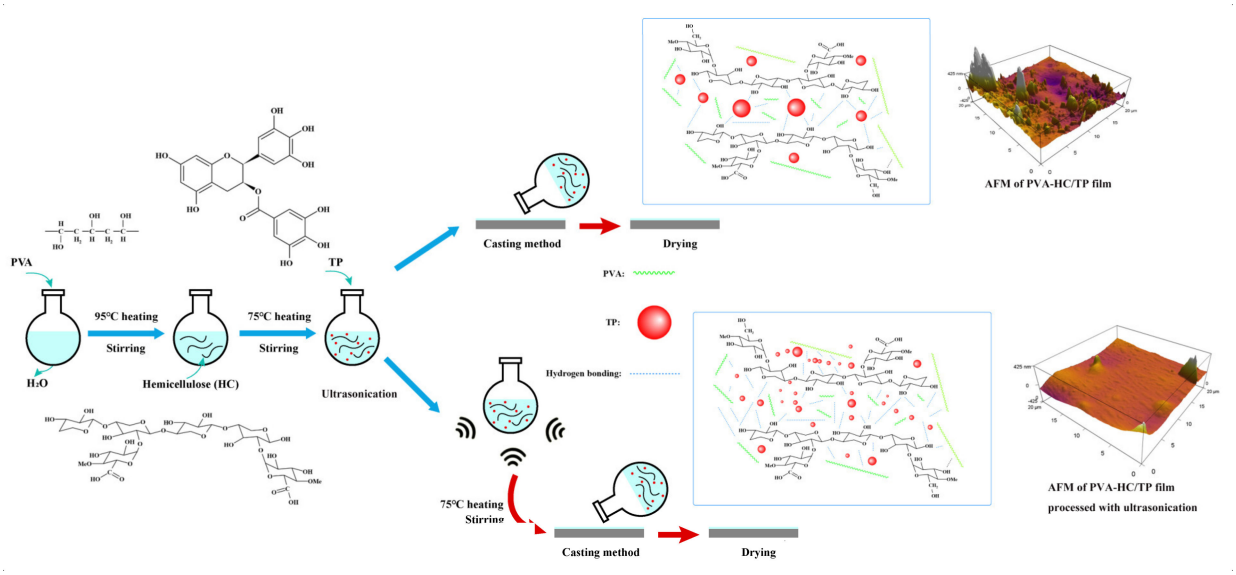

Scheme 1. Schematic illustration of film preparation process.

2.3. Film Characterization

2.3.1. Fourier Transform Infrared Spectroscopy (FT-IR) Analysis

The FTIR of the films was conducted on a Spectrum 10 spectrometer (PerkinElmer, Waltham, MA, USA) with 32 scans in a range from 400 to 4000 cm^{-1} at a resolution of 4 cm^{-1} using attenuated total reflectance mode.

2.3.2. Microstructure Analysis

Scanning electron microscopy (SEM) of the films was conducted on a JSM 7800 F (JEOL, Akishima, Japan). The films were coated with a thin layer of gold before measurement, and magnification was 5000×. The atomic force microscopy (AFM) of all films at the nano level was studied by Oxford Cypher (Oxford Instruments, UK) topographic (height) and phase images, which were recorded in tapping mode under ambient air.

2.3.3. X-ray Diffraction

X-ray diffraction (XRD) patterns were recorded in reflection mode in the angular range of 5° to 50° (2θ) in steps of 0.02° (2θ), and measurements were conducted on an XRD-7000 S X-ray diffractometer (Shimadzu, Kyoto, Japan).

2.3.4. Thermal Analysis

Thermal analysis was performed with thermogravimetric analysis (TGA) and derivative thermogravimetric analysis (DTGA) measured on a TGA-Q500 thermogravimetric analyzer (TA Instruments, New Castle, DE, USA). The apparatus was continually flushed with nitrogen and heated from 25 °C to 700 °C at a heating rate of 10 °C/min.

2.3.5. Color Parameters and Transparency

The film color parameters were measured on a SP64 integrating sphere spectrophotometer (X-RITE, Grand Rapids, MI, USA), L*; a* and b* parameters were measured by placing the

films on the surface of a standard white plate (L* standard = 95.02, a* standard = −1.08, and b* standard = 0.17), Color difference (ΔE^*) was calculated by Equation (1) as follows:

$$\Delta E = \sqrt{\Delta a^2 + \Delta b^2 + \Delta c^2} \quad (1)$$

The transparency of the films was measured on whiteness tester XT−48 BN (PNSHAR, Hangzhou, China).

2.3.6. Water-Vapor Permeability

Water-vapor transmission rate (WVT) of the samples was measured on a TSY-T1 permeability analyzer (Labthink, Jinan, China) at 38 °C and a relative humidity of 90%. Water-vapor permeability (WVP) was calculated by Equation (2) as follows:

$$WVP = 1.157 \times 10^{-9} \times \frac{WVT \times d}{\Delta p} \quad (2)$$

where *WVP* is water-vapor permeability (g/cm^{-1}·s·Pa), *WVT* is water-vapor transmission (g/m^2·24 h), *d* is film thickness (cm), and Δp (Pa) is the difference in partial water-vapor pressure between the two sides of each film sample.

2.3.7. Mechanical Properties

The tensile strength (TS) and elongation at break (E) of the films were evaluated according to ASTM D882-12 [36] using electronic tensile machine XLW-PC (Labthink, China). The sample was cut into strips (70 × 10 mm), and examined at a testing speed of 50 mm/min.

2.3.8. Antioxidant Activity

A DPPH free radical scavenging assay was carried out according to previous research with slight modifications [37]. To begin, 0.1 g film was dissolved into 20 mL distilled water. The mixture was then continuously stirred for 5 h in a water bath at 25 °C. Then, 1 mL of the solution removed from the released medium was mixed with 4 mL of DPPH methanol solution (75 μmol/L). To ensure full reaction for 12 h, the mixture was held in the dark and shaken discontinuously. The absorbance of the mixture was then measured at 517 nm on a UV1006 M031 UV–visible spectrometer (VARIAN, Palo Alto, CA, USA). The *DPPH* scavenging ratio was calculated by Equation (3) as follows:

$$DPPH = \frac{A_{DPPH} - A_S}{A_{DPPH}}, \quad (3)$$

where A_{DPPH} is the absorbance of the methanol solution, and A_S is the absorbance of the tested sample.

2.3.9. Statistical Analysis

The difference between factors and levels was evaluated by analysis of variance (IBM SPSS Statistics 24). All data are presented as mean ± standard deviation.

3. Results and Discussion

3.1. FT-IR Analysis

The FT-IR spectra of TP, TP1-0, TP1-45, TP10-0, TP10-45, and PVA/HC are shown in Figure 1. From the FT-IR spectrum of TP, bands at 1379 and 1640 cm^{-1} were ascribed to C-H and C=C, respectively. The band corresponding to the stretching vibrations of the hydroxyl group (–OH) was at about 3554 cm^{-1} [38]. For PVA-HC films, peaks at 1635 and 2928 cm^{-1} were attributed to the C=O stretching bands, the symmetric and asymmetric subsets of –CH_2– and the O–H stretching vibration for PVA-HC films located at 3430 cm^{-1} [39]. Compared with the PVA-HC films, the O–H stretching vibration absorption peaks of PVA-

HC-incorporated TP films moved to the low wavenumbers (redshift) of 3330 cm^{-1}, which indicated the new hydrogen bond formed between TP and the PVA–HC matrix. In addition, under the effect of ultrasonic treatment, the –OH bond was shifted from 3330 cm^{-1} for TP1-0 to 3319 cm^{-1} for TP1-45, which was attributed to a supermixing effect by ultrasonic action and intensified molecular motion [29,37]. Moreover, the band at 1638 cm^{-1} of TP10-0 was redshifted to 1609 cm^{-1} of TP10-45, which was ascribable to C=O stretching for TP and indicated PVA interacted with TP. From analysis of FT-IR results, the interaction was strengthened between TP and PVA-HC by ultrasonic action.

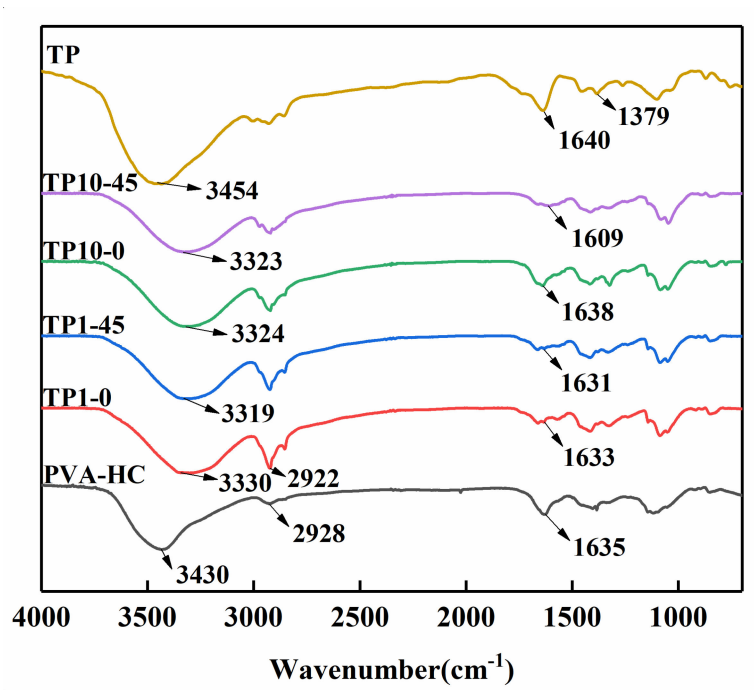

Figure 1. FT-IR of tea polyphenols (TP), poly (vinyl alcohol) (PVA)-hemicellulose (HC), and different mass ratios of PVA–HC/TP under different ultrasonic durations.

3.2. Microstructure Analysis

Scanning electron microscopy (SEM) was used for the study of the film microstructures shown in Figure 2. The untreated films (Figure 2b,d) exhibited phase separation in the PVA-HC/TP matrix with a rough surface. Figure 2c,e depicts the microstructure of PVA-HC/TP films processed with ultrasonication. Obviously, the surfaces of the ultrasound-treated films were smoother than those of the untreated films. This could be because the ultrasonic process may have helped to reduce TP agglomeration, leading to the reaction centers of TP being exposed, which made hydrogen bond cross-links form between the TP and the PVA-HC matrix. Abral et al. also found that ultrasound reduces the amount of incomplete gelatinized starch granules, which results in the formation of a film with a denser structure [40].

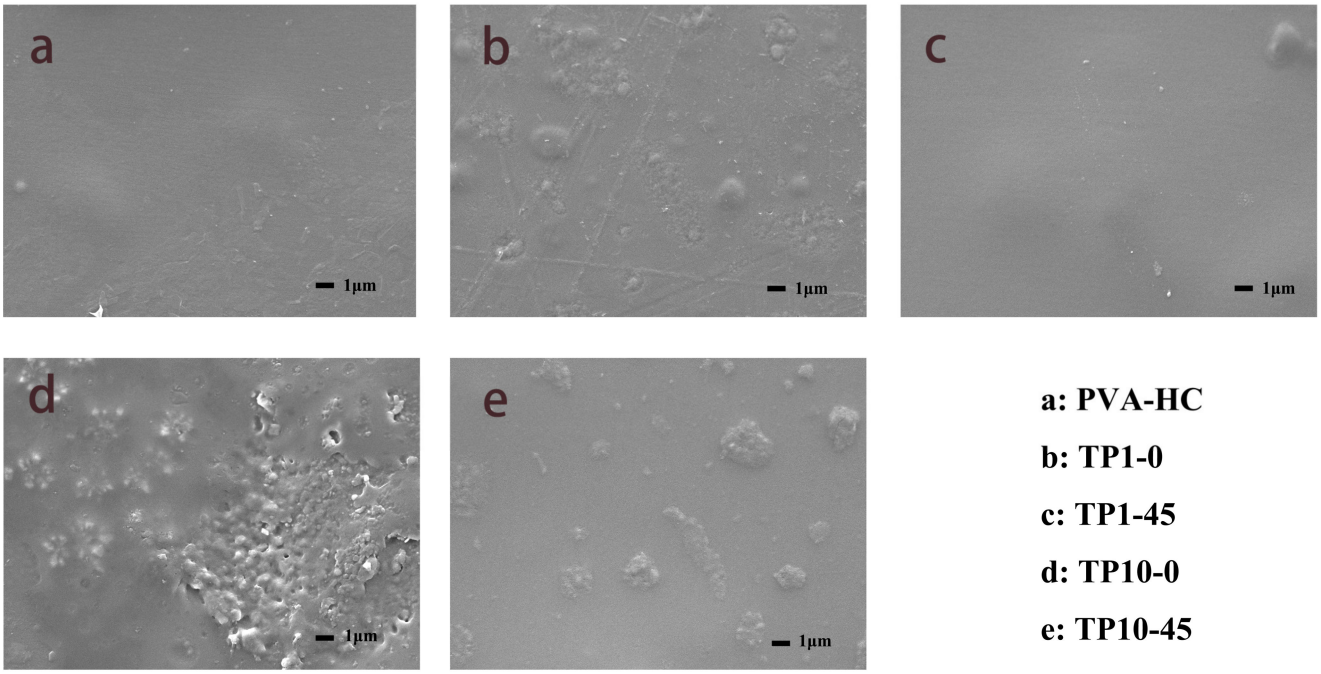

Figure 2. SEM images of PVA-HC and different mass ratios of PVA-HC/TP under different ultrasonic durations.

In order to better study the dispersion of TP in film, Figure 3 shows the 3D topographic image of samples measured by atomic force microscope (AFM). Figure 3a,c show that the surfaces of PVA-HC/TP films revealed many "sea-island" structures. In contrast, the AFM image of the films processed with ultrasonication (Figure 3b,d) shows that the surfaces are relatively smooth, compact, and homogeneous, which indicated that TP was well-distributed in the PVA-HC matrix, and that no critical agglomeration of TP was visible. A similar result was reported by Wu and coauthors, who observed that the untreated film surface was rough, while the surfaces of the films processed with ultrasonication were smooth and cohesive [41]. In this study, due to the disintegration of the TP agglomeration under intense ultrasonics in the film-forming solution, the film-forming components could be completely solubilized and hydrated, resulting in more homogeneous PVA-HC/TP film structure [42]. In addition, the Ra value was decreased from 84.666 nm for TP10-0 to 23.895 nm for TP10-45. Correspondingly, the results of SEM and AFM confirmed that TP and PVA-HC formed a dense network structure through ultrasound action.

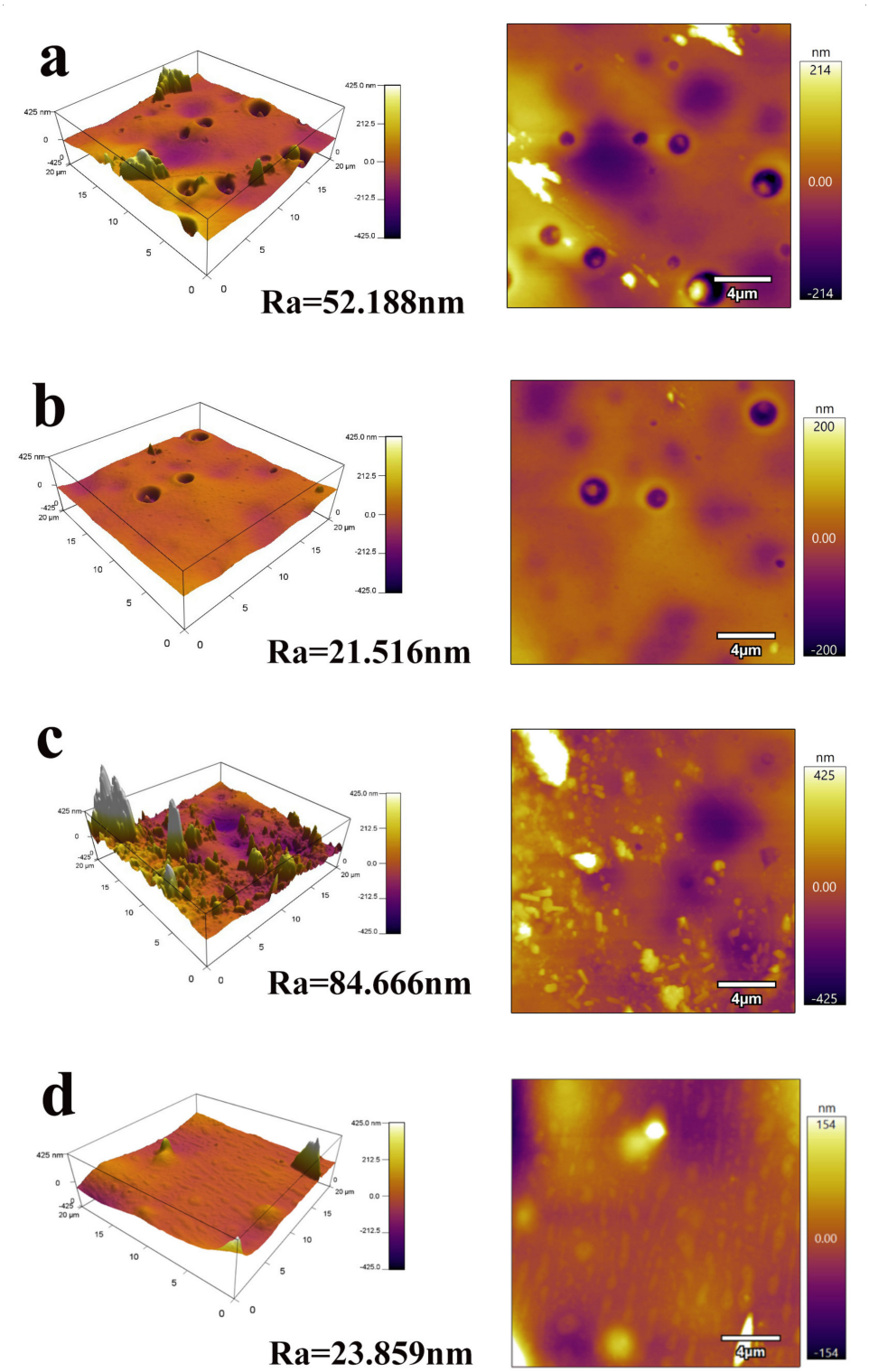

Figure 3. AFM images of different mass ratios of PVA-HC/TP under different ultrasonic durations: (**a**) TP1-0, (**b**) TP1-45, (**c**) TP10-0, (**d**) TP10-45.

3.3. X-ray Diffractometer Analysis

Figure 4 displays the diffraction patterns of ultrasonically treated and untreated samples. PVA is a typical semipartial crystalline polymer due to the presence of high numbers of physical interactions (like hydrogen) existing between the polymer chains [43]. The PVA-HC/TP without ultrasonic treatment showed the main characteristic peaks at $2\theta = 19.6°$ assigned to the (101) crystallographic plane, as well as one slight peak at a 2θ

of approximately 34.44°. When the PVA-HC/TP films were treated by ultrasonication, the crystal peak at 34.44° disappeared, indicating that the crystallinity of the film matrix was influenced. Similar results were found for acid-hydrolyzed waxy maize starch by Kim et al. [44]. As shown in Figure 4, the diffraction strength of the ultrasonically treated samples was lower compared to that of the treated samples. This could be due to the ultrasonic action breaks of certain noncovalent bonds between PVA-HC and TP in the film matrix, which suggest that the dispersibility of TP was increased, allowing for the formation of H bonds between TP and PVA-HC.

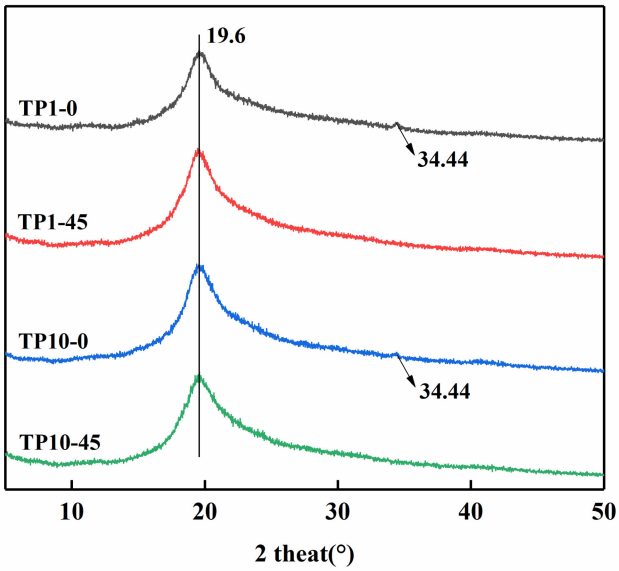

Figure 4. X-ray diffraction patterns of different mass ratios of PVA-HC/TP under different ultrasonic durations.

3.4. Thermogravimetric Analysis

TGA is considered an important technique for calculating the thermal stability of polymers. The thermal stability of the samples is demonstrated in Figure 5. The decomposition of the films was mainly observed in three stages. Approximately 10% of initial weight was lost in the first stage at a temperature of 80 to 140 °C because the absorbed water in the molecular chains of the sample was dehydrated [45,46]. The second stage from 230 to 370 °C corresponds to the degradation of the PVA-HC matrix and TP chains. The third stage of weight loss occurred above 370 °C, which was probably due to cleavage of the C–C backbone of the PVA and the carbonation of polymers [47]. As shown in Table 1, T_{onset} was shifted to the lower values as TP content increased due to the formation of TP agglomerates in the film matrix [48]. The maximal weight-loss temperature rose while TP content increased, which could mainly be attributed to the following reasons: First, the increase in TP content led to an increase in hydrogen bond cross-linking sites among TP, PVA, and HC; second, the large number of benzene ring groups in TP improve films' thermal stability. Similar results were also observed on lignin(aromatic ring compound)/PVA blend fibers [49]. Subsequently, the effects of ultrasonic treatment on the thermal stability of PVA-HC/TP films were investigated. The T_{onset} of the films increased with ultrasound intervention, which was a result of cross-linking between TP and the PVA-HC matrix. Due to hydrogen bond formation between TP and matrix with ultrasound treatment, the maximal thermal rate of decomposition with ultrasonication was from 286.89 °C in the TP10-0 films to 290.56 °C in the TP10-45 films.

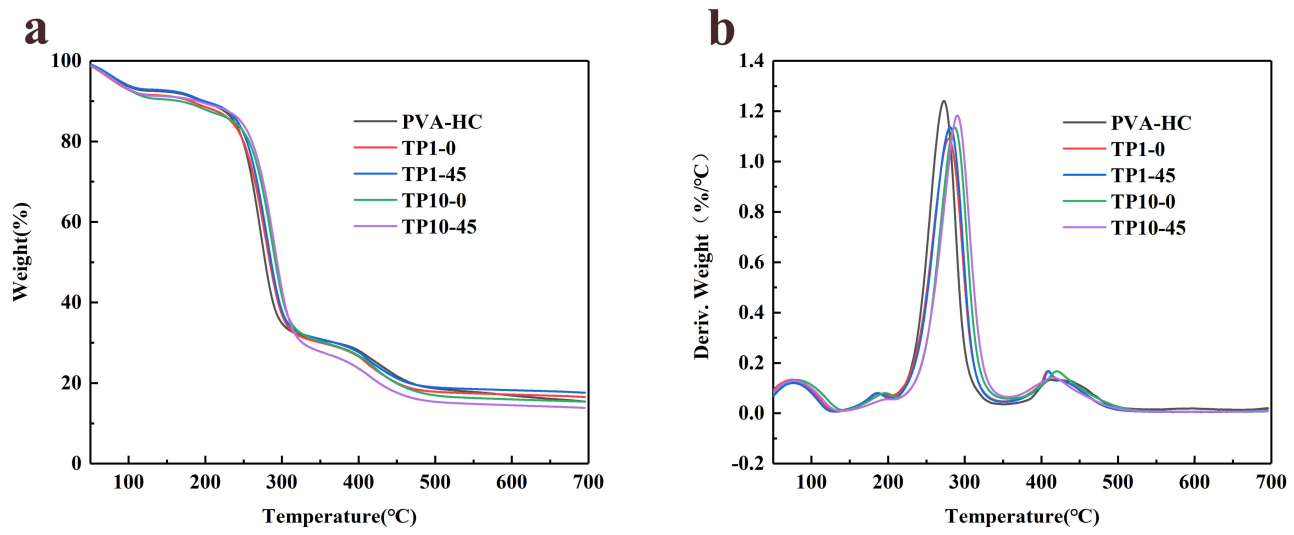

Figure 5. (**a**) TGA of different mass ratios of PVA-HC/TP under different ultrasonic duration; (**b**) DTGA different mass ratio of PVA-HC/TP under different ultrasonic duration.

Table 1. Thermal characteristics of obtained films.

Samples	T_{onset} (°C) [a]	T_{max} (°C) [b]	$T_{d50\%}$ (°C) [c]	$T_{d60\%}$ (°C) [d]
PVA–HC	195.28	273.19	278.27	288.51
TP1-0	180.42	278.51	284.33	295.02
TP1-45	198.65	281.22	286.13	296.72
TP10-0	162.98	286.89	291.47	301.97
TP10-45	188.72	290.56	293.72	303.64

[a]Thermal-decomposition temperature taken as onset of significant (5%) weight loss after initial moisture loss. [b] Temperature for corresponding maximal weight loss. [c] Temperature for corresponding 50% weight loss. [d] Temperature for corresponding 60% weight loss.

3.5. Color Parameters and Transparency

As shown in Figure 6, PVA-HC film was near transparent without any coloration. On the other hand, the transparency of the PVA-HC films that incorporated TP was decreased, with TP-incorporated films becoming red and yellow. Similar color-parameter changes were reported in starch/TP and PVA/TP films [37,50]. In addition, when PVA-HC/TP films were processed by ultrasonic treatment, the ΔE value was decreased ($p < 0.001$), which indicated that the homogeneity of the films was increased. Additionally, the transparency of ultrasonically treated samples was higher than that of the untreated sample ($p \leq 0.001$), which suggested that the film-forming compositions were made more consistent by ultrasonication. In general, the stronger the compatibility of the film's film-forming structure is, the greater light transmission it has. The above result can be attributed to film grain size and roughness being decreased by ultrasonic treatment, which led to light path blocking and reduced light scattering [51,52].

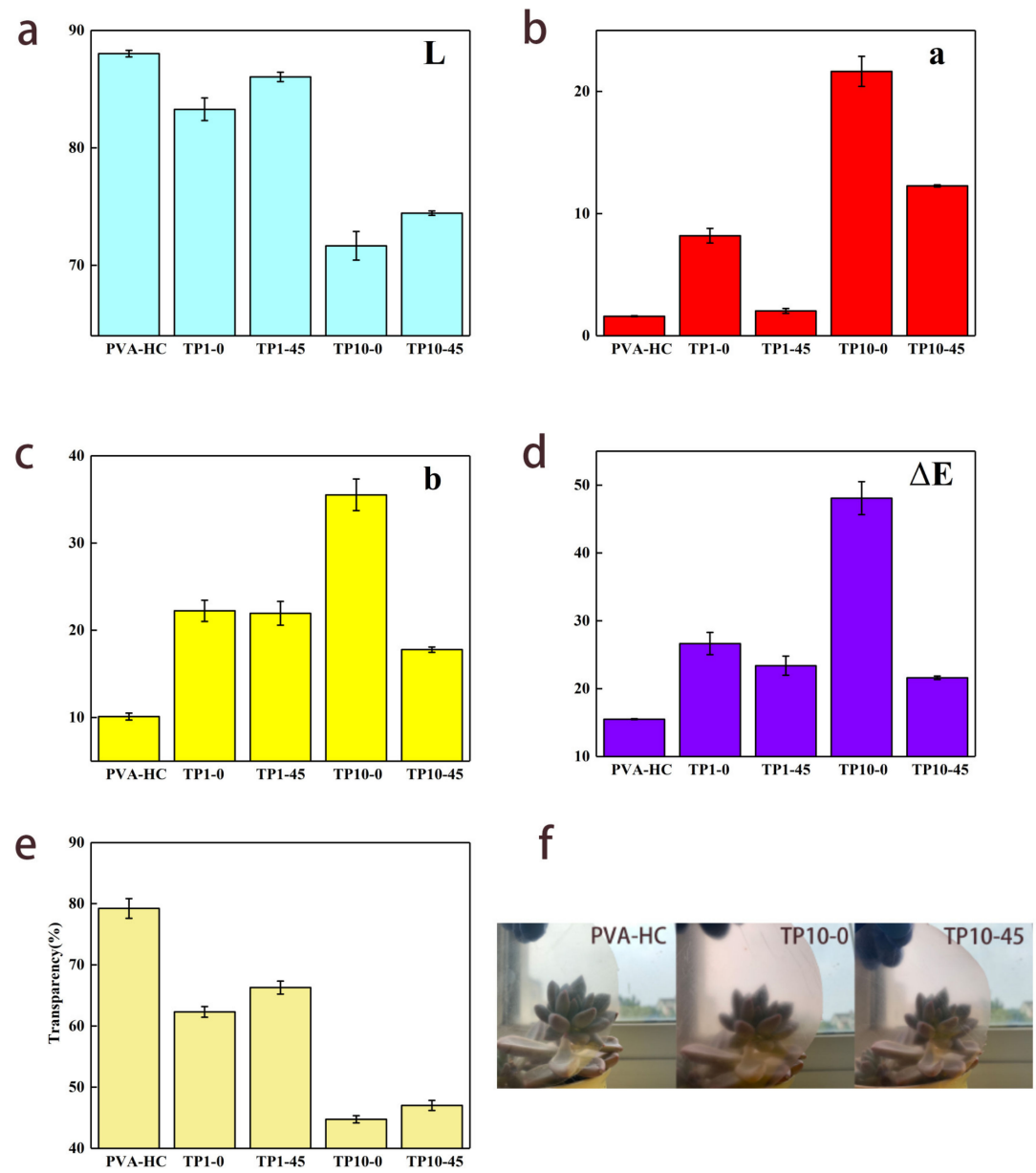

Figure 6. (**a**) L value, (**b**) a value, (**c**) b value, (**d**) ΔE value, (**e**) transparency, and (**f**) photographs of films.

3.6. DPPH Radical Scavenging Activity

Antioxidant packaging is a large category of active packaging and a very promising technique for extending the shelf life of food products [53]. Antioxidants changed the DPPH radical into a yellow diphenylpicrylhydrazine compound in this analysis, and the extent of this reaction depended heavily on the hydrogen-donating potential of the antioxidants [54]. The film without TP exhibited no scavenging behavior against free radical DPPH (not included in the graph), indicating that it did not exhibit antioxidant properties. Similarly, Zhou et al. reported the curdlan/chitosan film without tea polyphenols also exhibited no antioxidant capacity [27]. As shown in Figure 7, the free radical scavenging rates of the films were 4.46 ± 1.17% for the TP1-0 films, 44.20 ± 0.49% for the TP5-0 films, and 73.24 ± 1.01% for the TP10-0 films ($p < 0.001$). The TP10 films showed the highest DPPH radical scavenging activity relative to the other samples, indicating that the TP10 film showed excellent antioxidant capacity, consistent with previously reported chitosan/TP, gelatin/TP, and EVOH/TP films [55–57]. In addition, ultrasonic treatment had a certain effect on the antioxidant properties of the film to some degree. DPPH scavenging activity

was increased from 73.24 ± 1.01% for the TP10-0 films to 85.45 ± 1.21% for the TP10-45 films ($p < 0.001$). As described above, ultrasound treatment dramatically changed the physical and structural properties of the membrane. Some researchers stated that ultrasonic waves can loosen membrane network structures and facilitate the release of the active material [58]. Here, tea polyphenol was dispersed in the film matrix and loosened the film structure observed by SEM, AFM, and XRD, which made it easier to release active substances to increase the film's antioxidant capacity.

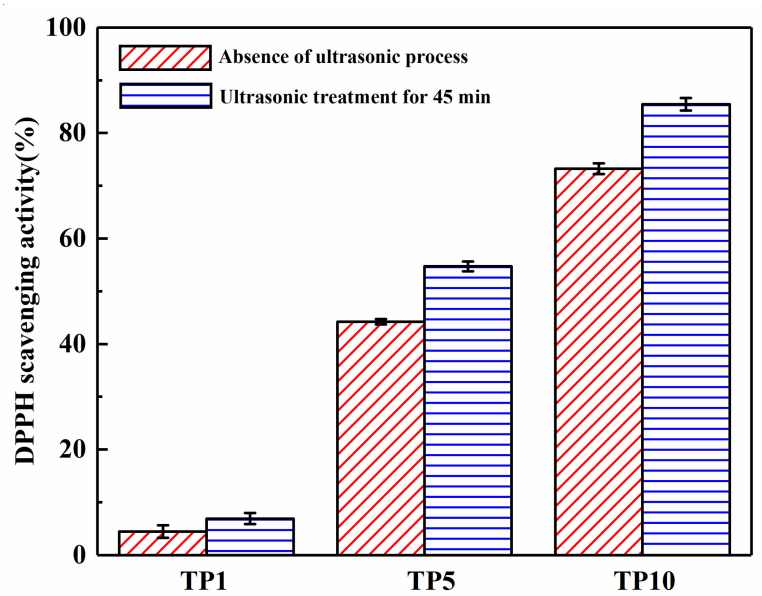

Figure 7. DPPH scavenging activity of samples with different TP content and ultrasound existence.

3.7. Water Vapor Barrier Properties

The effects of adding various amounts of TP and ultrasonic length concentrations on the WVP of the films is illustrated in Figure 8 compared with neat PVA/hemicellulose(Xylan) films by a previous report (WVP:320 × 10^{-12}(g·cm/cm^2·s·Pa)) [59]. PVA-HC/TP films showed a lower WVP value. Moreover, the water-vapor barrier performance of the films was increased with the extension of ultrasound duration; WVP value decreased from 6.41 ± 0.21 (×10^{-12} g·cm/cm^2·s·Pa) for the TP10-0 films to 4.29 ± 0.14 (×10^{-12} g·cm/cm^2·s·Pa) for the TP10-45 films ($p < 0.001$). The improved barrier properties were likely because of the "torturous path effect" [60,61]. Water molecules are likely to follow the direction with the least resistance in the water-vapor transmission process. In this research, we concluded that two factors played a crucial role in reducing the WVP of the films. First, the large number of hydrophobic benzene ring groups in TP diminished the infiltration capacity against water molecules. Second, tea polyphenols were dispersed into micro–nano particles under the action of the ultrasound, as shown in AFM, which formed the hydrogen bond cross-linking in the film matrix. Thus, the water-vapor barrier properties of the PVA–HC/TP films were greatly improved.

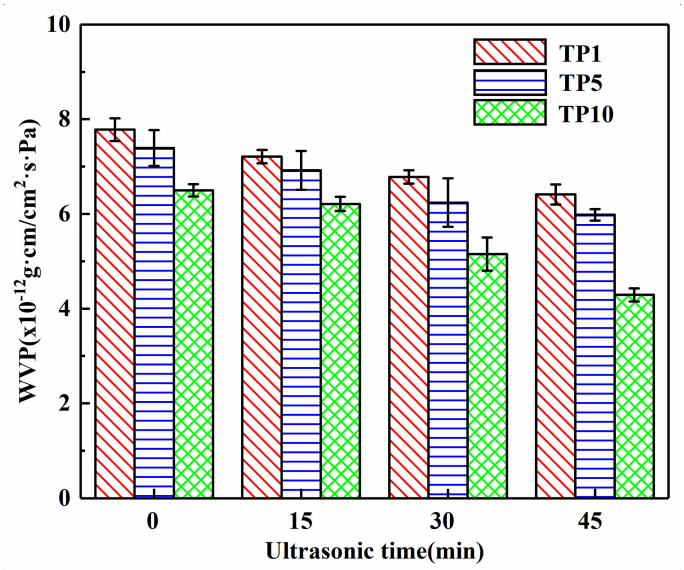

Figure 8. Water-vapor permeability on different mass ratios of PVA-HC/TP with different ultrasonic durations.

3.8. Mechanical Properties

Figure 9 demonstrates the effects of different TP contents and ultrasonic length concentrations on the mechanical properties of the films. The tensile strength of the film depends on the distribution and density of inter- and intramolecular interactions of the polymer matrix [62]. In this study, the tensile strength (TS) of the films declined as TP concentration increased. On the other hand, the introduction of TP could reduce the flexibility of the films, leading to a lower elongation at break (E) of the films. Figure 9 shows that the TS value was increased from 18.57 ± 0.85 Mpa for the TP10-15 films to 25.61 ± 0.53 Mpa for the TP10-45 films ($p < 0.001$). Changes in TS were possibly due to the configuration of the micronetwork and the intermolecular force in the film matrix resulting from the hydrogen-bond interaction between TP and PVA-HC. In contrast, elongation at break of films decreased dramatically under the influence of the ultrasound, attributed to the hydrogen bonding force between tea polyphenols and film matrix restricting the movement of the molecular chain during stretching.

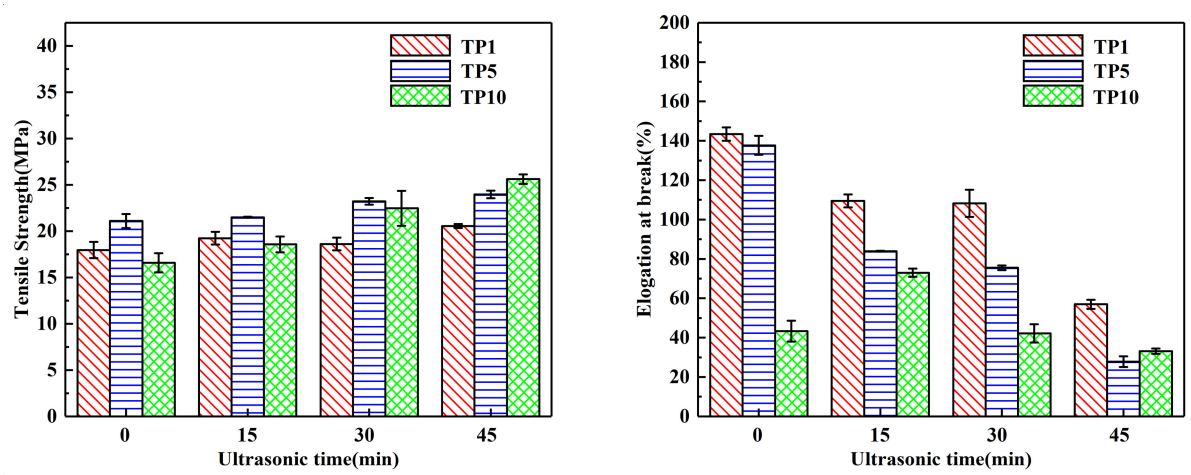

Figure 9. Tensile strength and elongation at break on different mass ratios of PVA-HC/TP with different ultrasonic durations.

4. Conclusions

In summary, the preparation of active poly(vinyl alcohol)-hemicellulose (HC) with tea polyphenol (TP) films via ultrasound assistance was described. Specifically, the effects of TP addition and ultrasonication on the physicochemical properties of films were investigated. FTIR, SEM, and AFM indicated good miscibility between the film matrix and TP due to the formation of hydrogen bonding in the ultrasonic process. According to TGA/DTGA analysis, ultrasonication could develop the thermal stability of composite films, as the DPPH scavenging activity of TP10 films was significantly improved from 73.24% to 85.45% as ultrasonic duration increased from 0 to 45 min. In addition, mechanical tests and water-vapor permeability indicated that the tensile strength and water-vapor barrier performance of the composite films increased as the duration of ultrasonic treatment extended. The above results implied that the PVA-HC/TP films have potential applications as active film in food packaging. More importantly, this work adds to the literature as it illustrates the positive effects of ultrasonic processing on the properties of polysaccharide-based active packaging materials.

Supplementary Materials: The following are available online at https://www.mdpi.com/2079-6412/11/2/219/s1, Table S1: The composition of each formulation of films.

Author Contributions: Investigation, software, writing—original draft, Y.W.; formal analysis, J.L.; software, X.G.; supervision, F.Q. and H.W.; supervision, funding acquisition, writing—review and editing, Y.L. All authors have read and agreed to the published version of the manuscript.

Funding: This research was funded by National Key R&D Program of China, grant number 2018YFD0400703; Scientific Research Project of Liaoning Provincial Department of Education, grant number J2020040; and State Key Laboratory of Pulp and Paper Engineering, grant number 201802.

Institutional Review Board Statement: Not applicable.

Informed Consent Statement: Not applicable.

Data Availability Statement: The study did not report any data.

Conflicts of Interest: The authors declare no conflict of interest.

References

1. Kessenich, B.L.; Pokhrel, N.; Kibue, J.K.; Flury, M.; Maibaum, L.; De Yoreo, J.J. Negatively Charged Lipids Exhibit Negligible Effects on the Water Repellency of Montmorillonite Films. *ACS Omega* **2020**, *5*, 12154–12161. [CrossRef] [PubMed]
2. Piñeros-Hernandez, D.; Medina-Jaramillo, C.; López-Córdoba, A.; Goyanes, S. Edible cassava starch films carrying rosemary antioxidant extracts for potential use as active food packaging. *Food Hydrocoll.* **2017**, *63*, 488–495. [CrossRef]
3. Medina-Jaramillo, C.; Ochoa-Yepes, O.; Bernal, C.; Famá, L. Active and smart biodegradable packaging based on starch and natural extracts. *Carbohydr. Polym.* **2017**, *176*, 187–194. [CrossRef] [PubMed]
4. Zhang, X.; Xiao, N.; Chen, M.; Wei, Y.; Liu, C. Functional packaging films originating from hemicelluloses laurate by direct transesterification in ionic liquid. *Carbohydr. Polym.* **2020**, *229*, 115336. [CrossRef]
5. Zhao, Y.; Sun, H.; Yang, B.; Weng, Y.-X. Hemicellulose-Based Film: Potential Green Films for Food Packaging. *Polymers* **2020**, *12*, 1775. [CrossRef] [PubMed]
6. Zhang, S.; Xia, C.; Dong, Y.; Yan, Y.; Li, J.; Shi, S.Q.; Cai, L. Soy protein isolate-based films reinforced by surface modified cellulose nanocrystal. *Ind. Crop. Prod.* **2016**, *80*, 207–213. [CrossRef]
7. Deutschmann, R.; Dekker, R.F. From plant biomass to bio-based chemicals: Latest developments in xylan research. *Biotechnol. Adv.* **2012**, *30*, 1627–1640. [CrossRef] [PubMed]
8. Mamman, A.S.; Lee, J.-M.; Kim, Y.-C.; Hwang, I.T.; Park, N.-J.; Hwang, Y.K.; Chang, J.-S.; Hwang, J.-S. Furfural: Hemicellulose/xylosederived biochemical. *Biofuels Bioprod. Biorefining* **2008**, *2*, 438–454. [CrossRef]
9. Kobayashi, S.; Kashiwa, K.; Kawasaki, T.; Shoda, S. Novel method for polysaccharide synthesis using an enzyme: The first in vitro synthesis of cellulose via a nonbiosynthetic path utilizing cellulase as catalyst. *J. Am. Chem. Soc.* **1991**, *113*, 3079–3084. [CrossRef]
10. Kayserilioğlu, B.S.; Bakir, U.; Yilmaz, L.; Akkaş, N. Use of xylan, an agricultural by-product, in wheat gluten based biodegradable films: Mechanical, solubility and water vapor transfer rate properties. *Bioresour. Technol.* **2003**, *87*, 239–246. [CrossRef]
11. Li, N.; Liu, Z.; Xu, S. Dynamically formed poly (vinyl alcohol) ultrafiltration membranes with good anti-fouling characteristics. *J. Membr. Sci.* **2000**, *169*, 17–28. [CrossRef]
12. Mali, S.; Debiagi, F.; Grossmann, M.V.; Yamashita, F. Starch, sugarcane bagasse fibre, and polyvinyl alcohol effects on extruded foam properties: A mixture design approach. *Ind. Crop. Prod.* **2010**, *32*, 353–359. [CrossRef]

13. Heikkinen, S.L.; Mikkonen, K.S.; Koivisto, P.; Heikkilä, M.I.; Pirkkalainen, K.; Liljeström, V.; Serimaa, R.; Tenkanen, M. Long-term physical stability of plasticized hemicellulose films. *BioResources* **2014**, *9*, 906–921. [CrossRef]
14. Abral, H.; Atmajaya, A.; Mahardika, M.; Hafizulhaq, F.; Handayani, D.; Sapuan, S.; Ilyas, R. Effect of ultrasonication duration of polyvinyl alcohol (PVA) gel on characterizations of PVA film. *J. Mater. Res. Technol.* **2020**, *9*, 2477–2486. [CrossRef]
15. Wang, S.; Ren, J.; Kong, W.; Gao, C.; Liu, C.; Peng, F.; Sun, R. Influence of urea and glycerol on functional properties of biodegradable PVA/xylan composite films. *Cellulose* **2013**, *21*, 495–505. [CrossRef]
16. Wang, S.; Ren, J.; Li, W.; Sun, R.; Liu, S. Properties of polyvinyl alcohol/xylan composite films with citric acid. *Carbohydr. Polym.* **2014**, *103*, 94–99. [CrossRef]
17. Shao, H.; Sun, H.; Yang, B.; Zhang, H.; Hu, Y. Facile and green preparation of hemicellulose-based film with elevated hydrophobicity via cross-linking with citric acid. *RSC Adv.* **2019**, *9*, 2395–2401. [CrossRef]
18. Wu, H.; Lei, Y.; Zhu, R.; Zhao, M.; Lu, J.; Xiao, D.; Jiao, C.; Zhang, Z.; Shen, G.; Li, S. Preparation and characterization of bioactive edible packaging films based on pomelo peel flours incorporating tea polyphenol. *Food Hydrocoll.* **2019**, *90*, 41–49. [CrossRef]
19. Sui, W.; Xiao, Y.; Liu, R.; Wu, T.; Zhang, M. Steam explosion modification on tea waste to enhance bioactive compounds' extractability and antioxidant capacity of extracts. *J. Food Eng.* **2019**, *261*, 51–59. [CrossRef]
20. Osman, A. Multiple pathways of the reaction of 2,2-diphenyl-1-picrylhydrazyl radical (DPPH) with (+)-catechin: Evidence for the formation of a covalent adduct between DPPH and the oxidized form of the polyphenol. *Biochem. Biophys. Res. Commun.* **2011**, *412*, 473–478. [CrossRef]
21. Feng, L.; Jiang, T.; Wang, Y.; Li, J. Effects of tea polyphenol coating combined with ozone water washing on the storage quality of black sea bream (Sparus macrocephalus). *Food Chem.* **2012**, *135*, 2915–2921. [CrossRef]
22. Bora, A.F.M.; Ma, S.; Li, X.; Liu, L. Application of microencapsulation for the safe delivery of green tea polyphenols in food systems: Review and recent advances. *Food Res. Int.* **2018**, *105*, 241–249. [CrossRef] [PubMed]
23. Yang, H.-J.; Lee, J.-H.; Won, M.; Bin Song, K. Antioxidant activities of distiller dried grains with solubles as protein films containing tea extracts and their application in the packaging of pork meat. *Food Chem.* **2016**, *196*, 174–179. [CrossRef] [PubMed]
24. Wang, L.; Dong, Y.; Men, H.; Tong, J.; Zhou, J. Preparation and characterization of active films based on chitosan incorporated tea polyphenols. *Food Hydrocoll.* **2013**, *32*, 35–41. [CrossRef]
25. Liu, F.; Avena-Bustillos, R.J.; Chiou, B.-S.; Li, Y.; Ma, Y.; Williams, T.G.; Wood, D.F.; McHugh, T.H.; Zhong, F. Controlled-release of tea polyphenol from gelatin films incorporated with different ratios of free/nanoencapsulated tea polyphenols into fatty food simulants. *Food Hydrocoll.* **2017**, *62*, 212–221. [CrossRef]
26. Gao, H.-X.; He, Z.; Sun, Q.; He, Q.; Zeng, W.-C. A functional polysaccharide film forming by pectin, chitosan, and tea polyphenols. *Carbohydr. Polym.* **2019**, *215*, 1–7. [CrossRef] [PubMed]
27. Zhou, Y.; Xu, T.; Zhang, Y.; Zhang, C.; Lu, Z.; Lu, F.; Zhao, H. Effect of Tea Polyphenols on Curdlan/Chitosan Blending Film Properties and Its Application to Chilled Meat Preservation. *Coatings* **2019**, *9*, 262. [CrossRef]
28. Shao, X.; Sun, H.; Jiang, R.; Yu, Y. Physical and antibacterial properties of corn distarch phosphate/carboxymethyl cellulose composite films containing tea polyphenol. *J. Food Process. Preserv.* **2020**, *44*, e14401. [CrossRef]
29. Liu, Y.; Wang, S.; Lan, W.; Qin, W. Development of ultrasound treated polyvinyl alcohol/tea polyphenol composite films and their physicochemical properties. *Ultrason. Sonochem.* **2019**, *51*, 386–394. [CrossRef]
30. Mallakpour, S.; Darvishzadeh, M. Ultrasonic treatment as recent and environmentally friendly route for the synthesis and characterization of polymer nanocomposite having PVA and biosafe BSA-modified ZnO nanoparticles. *Polym. Adv. Technol.* **2018**, *29*, 2174–2183. [CrossRef]
31. Albano, K.M.; Nicoletti, V.R. Ultrasound impact on whey protein concentrate-pectin complexes and in the O/W emulsions with low oil soybean content stabilization. *Ultrason. Sonochem.* **2018**, *41*, 562–571. [CrossRef]
32. Wang, L.; Ding, J.; Fang, Y.; Pan, X.; Fan, F.; Li, P.; Hu, Q. Effect of ultrasonic power on properties of edible composite films based on rice protein hydrolysates and chitosan. *Ultrason. Sonochem.* **2020**, *65*, 105049. [CrossRef]
33. Liu, P.; Wang, R.; Kang, X.; Cui, B.; Yu, B. Effects of ultrasonic treatment on amylose-lipid complex formation and properties of sweet potato starch-based films. *Ultrason. Sonochem.* **2018**, *44*, 215–222. [CrossRef] [PubMed]
34. Xie, Y.; Ma, Z.; Lv, Y.; Wang, Q. Influence of Urea and Sorbitol on Packaging Properties of Biodegradable PVA/Hemicellulose Blend Films. In Proceedings of the 21st IAPRI World Conference on Packaging, Zhuhai, China, 19–22 June 2018.
35. Xie, Y.; Guo, X.; Ma, Z.; Gong, J.; Wang, H.; Lv, Y. Efficient Extraction and Structural Characterization of Hemicellulose from Sugarcane Bagasse Pith. *Polymers* **2020**, *12*, 608. [CrossRef] [PubMed]
36. ASTM International. *ASTM D882: Standard Test Method for Tensile Properties of Thin Plastic Sheeting*; ASTM Standard; ASTM International: West Conshohocken, PA, USA, 2012; Volume 12. [CrossRef]
37. Chen, C.; Tang, Z.; Ma, Y.; Qiu, W.; Yang, F.; Mei, J.; Xie, J. Physicochemical, microstructural, antioxidant and antimicrobial properties of active packaging films based on poly(vinyl alcohol)/clay nanocomposite incorporated with tea polyphenols. *Prog. Org. Coatings* **2018**, *123*, 176–184. [CrossRef]
38. Yu, S.-H.; Tsai, M.-L.; Lin, B.-X.; Lin, C.-W.; Mi, F.-L. Tea catechins-cross-linked methylcellulose active films for inhibition of light irradiation and lipid peroxidation induced β-carotene degradation. *Food Hydrocoll.* **2015**, *44*, 491–505. [CrossRef]
39. Xiao, S.; Gao, R.; Gao, L.; Li, J. Poly(vinyl alcohol) films reinforced with nanofibrillated cellulose (NFC) isolated from corn husk by high intensity ultrasonication. *Carbohydr. Polym.* **2016**, *136*, 1027–1034. [CrossRef] [PubMed]

40. Abral, H.; Basri, A.; Muhammad, F.; Fernando, Y.; Hafizulhaq, F.; Mahardika, M.; Sugiarti, E.; Sapuan, S.; Ilyas, R.; Stephane, I. A simple method for improving the properties of the sago starch films prepared by using ultrasonication treatment. *Food Hydrocoll.* **2019**, *93*, 276–283. [CrossRef]
41. Wu, F.; Zhou, Z.; Liang, M.; Zhong, L.; Xie, F. Ultrasonication Improves the Structures and Physicochemical Properties of Cassava Starch Films Containing Acetic Acid. *Starch Stärke* **2021**, *73*. [CrossRef]
42. Cheng, W.; Chen, J.; Liu, D.; Ye, X.; Ke, F. Impact of ultrasonic treatment on properties of starch film-forming dispersion and the resulting films. *Carbohydr. Polym.* **2010**, *81*, 707–711. [CrossRef]
43. Zhao, X.; Zhang, Q.; Chen, D.; Lu, P. Enhanced Mechanical Properties of Graphene-Based Poly(vinyl alcohol) Composites. *Macromolecules* **2010**, *43*, 2357–2363. [CrossRef]
44. Kim, H.-Y.; Han, J.-A.; Kweon, D.-K.; Park, J.-D.; Lim, S.-T. Effect of ultrasonic treatments on nanoparticle preparation of acid-hydrolyzed waxy maize starch. *Carbohydr. Polym.* **2013**, *93*, 582–588. [CrossRef] [PubMed]
45. Liu, X.; Chen, X.; Ren, J.; Chang, M.; He, B.; Zhang, C. Effects of nano-ZnO and nano-SiO_2 particles on properties of PVA/xylan composite films. *Int. J. Biol. Macromol.* **2019**, *132*, 978–986. [CrossRef] [PubMed]
46. Li, Y.; Li, J.; Li, Y.; Li, Y.; Song, Y.; Niu, S.; Li, N. Ultrasonic-assisted preparation of graphene oxide carboxylic acid polyvinyl alcohol polymer film and studies of thermal stability and surface resistivity. *Ultrason. Sonochem.* **2018**, *40*, 798–807. [CrossRef] [PubMed]
47. Holland, B.; Hay, J. The thermal degradation of poly(vinyl alcohol). *Polymer* **2001**, *42*, 6775–6783. [CrossRef]
48. Pandele, A.M.; Constantinescu, A.; Radu, I.C.; Miculescu, F.; Voicu, S.I.; Ciocan, L.T. Synthesis and Characterization of PLA-Micro-structured Hydroxyapatite Composite Films. *Materials* **2020**, *13*, 274. [CrossRef]
49. Kubo, S.; Kadla, J.F. The Formation of Strong Intermolecular Interactions in Immiscible Blends of Poly(vinyl alcohol) (PVA) and Lignin. *Biomacromolecules* **2003**, *4*, 561–567. [CrossRef]
50. Feng, M.; Yu, L.; Zhu, P.; Zhou, X.; Liu, H.; Yang, Y.; Zhou, J.; Gao, C.; Bao, X.; Chen, P. Development and preparation of active starch films carrying tea polyphenol. *Carbohydr. Polym.* **2018**, *196*, 162–167. [CrossRef]
51. Thanh, D.T.; Ko, K.B.; Khurelbaatar, Z.; Choi, C.-J.; Hong, C.-H.; Cuong, T.V. Transparent and flexible ultraviolet photoconductors based on solution-processed graphene quantum dots on reduced graphene oxide films. *Mater. Res. Bull.* **2017**, *91*, 49–53. [CrossRef]
52. Farmahini-Farahani, M.; Xiao, H.; Khan, A.; Pan, Y.; Yang, Y. Preparation and Characterization of Exfoliated PHBV Nanocomposites to Enhance Water Vapor Barriers of Calendared Paper. *Ind. Eng. Chem. Res.* **2015**, *54*, 11277–11284. [CrossRef]
53. Gómez-Estaca, J.; Montero, P.; Gómez-Guillén, M.C. Shrimp (Litopenaeus vannamei) muscle proteins as source to develop edible films. *Food Hydrocoll.* **2014**, *41*, 86–94. [CrossRef]
54. Gaikwad, K.K.; Lee, J.Y.; Lee, Y.S. Development of polyvinyl alcohol and apple pomace bio-composite film with antioxidant properties for active food packaging application. *J. Food Sci. Technol.* **2016**, *53*, 1608–1619. [CrossRef] [PubMed]
55. De Dicastillo, C.L.; Neriín, C.; Alfaro, P.; Catalaá, R.; Gavara, R.; Hernaández-Munñoz, P. Development of New Antioxidant Active Packaging Films Based on Ethylene Vinyl Alcohol Copolymer (EVOH) and Green Tea Extract. *J. Agric. Food Chem.* **2011**, *59*, 7832–7840. [CrossRef] [PubMed]
56. Wu, J.; Liu, H.; Ge, S.; Wang, S.; Qin, Z.; Chen, L.; Zheng, Q.; Liu, Q.; Zhang, Q. The preparation, characterization, antimicrobial stability and in vitro release evaluation of fish gelatin films incorporated with cinnamon essential oil nanoliposomes. *Food Hydrocoll.* **2015**, *43*, 427–435. [CrossRef]
57. Wrona, M.; Cran, M.J.; Nerín, C.; Bigger, S.W. Development and characterisation of HPMC films containing PLA nanoparticles loaded with green tea extract for food packaging applications. *Carbohydr. Polym.* **2017**, *156*, 108–117. [CrossRef] [PubMed]
58. Wang, D.; Lv, R.; Ma, X.; Zou, M.; Wang, W.; Yan, L.; Ding, T.; Ye, X.; Liu, D. Lysozyme immobilization on the calcium alginate film under sonication: Development of an antimicrobial film. *Food Hydrocoll.* **2018**, *83*, 1–8. [CrossRef]
59. Chen, X.; Ren, J.; Meng, L. Influence of Ammonium Zirconium Carbonate on Properties of Poly(vinyl alcohol)/Xylan Composite Films. *J. Nanomater.* **2015**, *2015*, 1–8. [CrossRef]
60. Liu, S.; Cai, P.; Li, X.; Chen, L.; Li, L.; Li, B. Effect of film multi-scale structure on the water vapor permeability in hydroxypropyl starch (HPS)/Na-MMT nanocomposites. *Carbohydr. Polym.* **2016**, *154*, 186–193. [CrossRef]
61. Sangermano, M.; Periolatto, M.; Signore, V.; Spena, P.R. Improvement of the water-vapor barrier properties of an uv-cured epoxy coating containing graphite oxide nanoplatelets. *Prog. Org. Coatings* **2017**, *103*, 152–155. [CrossRef]
62. Shankar, S.; Teng, X.; Li, G.; Rhim, J.-W. Preparation, characterization, and antimicrobial activity of gelatin/ZnO nanocomposite films. *Food Hydrocoll.* **2015**, *45*, 264–271. [CrossRef]